Strength Measurement of Optical Fibers by Bending

M. JOHN MATTHEWSON*,* and CHARLES R. KURKJIAN*

AT&T Bell Laboratories, Murray Hill, New Jersey 07974

SURESH T. GULATI*

Corning Glass Works, Corning, New York 14831

A bending technique for the strength measurement of glass fibers is described and an analysis is presented which determines the effective tested length as a function of the statistical parameters which describe the fracture properties of the fiber. The analysis is used to compare strength data determined in both tension and bending for various representative fibers. It is found that the tensile strength cannot be predicted from the strength in bending and vice versa because the tested lengths differ by at least 3 orders of magnitude. Thus, while bending does not replace tension as a measurement technique, it does provide additional valuable information about the flaw size distribution.

I. Introduction

THE strength of glass fiber can be determined by a tensile technique in which a length of fiber is gripped at each end and pulled in tension until it fails. The technique provides the failure load from which the failure stress can readily be calculated and either of these quantities is commonly used as a realistic measure of fiber strength for design purposes.

An alternative method of bending the fiber may be used since the strength determines the radius of curvature at fracture. A loop[1] or knot[2] test may be used, but these tests suffer from the disadvantage that the size of the loop or knot at fracture is difficult to determine. Also, a bare fiber will sustain damage by rubbing against itself. A bending method, first described in detail by France *et al.*,[3] which avoids these problems is critically examined here. Shown schematically in Fig. 1, it involves constraining a bent loop of fiber between two ground and polished faceplates which are then brought together until the fiber breaks. The fiber is held symmetrically between the faceplates by clamping to the guide plate. Alternatively the fiber can be held by grooves in the faceplate but this arrangement may not be suitable for bare fibers as the unprotected fiber surface may be severely damaged by contact with the edge and bottom of the groove (which is not easily polished to a smooth enough surface) leading to fracture at the faceplates rather than in the bent section.

The faceplates are brought together by a computer-controlled stepper motor which is halted when the fiber fracture is sensed by an acoustic detector. The failure strain is then calculated from the guide plate separation at fracture and the fiber diameter.

Bending has several attractive features and advantages over tensile testing:

(i) There are no gripping problems. Fibers with a compliant coating (e.g., silicone) or a degraded (e.g., by heat or water) higher modulus coating cannot easily be gripped in tension. Fibers, whether coated or uncoated, can readily be broken in bending, though for reasons of accuracy it may be advisable to strip any coating material.

(ii) The strength of a fiber whose tested section is stronger than its gripped section cannot be tested in tension. This situation can occur, for example, when investigating the strength of fibers at liquid-nitrogen temperatures since it is not simple to cool the grips.

(iii) Only a small length of fiber is subjected to stress; therefore, it is easy to "zero in" on a region of interest if it is small.

(iv) The bending technique is readily made highly accurate (in a relative sense, see below for absolute accuracy); it is easier to accurately measure the separation of the faceplates than the analogue output of a load cell. The faceplate separation at fracture is typically $\approx$2000 μm for a high-strength fiber and the accuracy to which this is determined is the step length of the stepper motor. A 1-μm stepper motor was used in this work—a 0.1-μm stepper motor could be used for higher accuracy but the maximum achievable loading rate (faceplate velocity) is proportionately lower.

(v) The system is easily computerized, the components are readily available and inexpensive, and the apparatus is compact and simple to use.

(vi) The fiber can easily be immersed in an environment. Liquid-nitrogen strengths have been found with comparative ease. Alternatively a gaseous or liquid environment can be blown or dripped on the small section of fiber under test, obviating the need for an environmental chamber. If the gas or liquid stream is directed toward the compressive side of the bent fiber, there is little risk of damage by impact with particulate contaminants influencing the results.

(vii) Since only a small length of fiber is under a high stress, only a small length of fiber disintegrates into dust at fracture. The fiber diameter close to the fracture can then be measured.

(viii) Only a small length of fiber ($\approx$3 cm) is used. This is clearly an advantage if only small quantities of fiber are available.

However, there are some problems with the bending technique.

(i) Absolute accuracy may not be as good as in tension since it is difficult to accurately determine the position of zero separation of the faceplates. Also, the overall fiber diameter is subtracted from the faceplate separation before calculation of the fracture strength and this can give significant errors for coated fibers since the coating thickness and concentricity can be variable, but more importantly, the coating can deform under the contact stresses thus

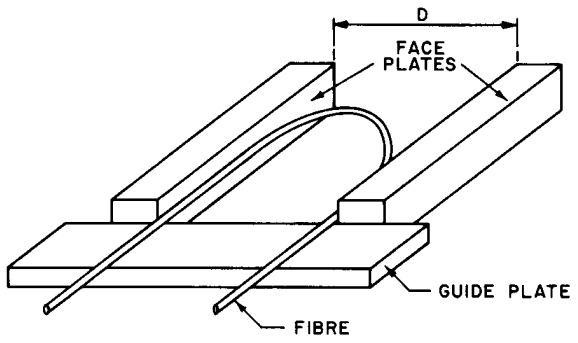

Fig. 1. Schematic diagram of the bending technique for breaking fibers.

Presented at the Glass Division Fall Meeting of the American Ceramic Society, October 19, 1984 (Paper No. 59-G-84F). Received December 19, 1985; revised copy received June 2, 1986; approved June 8, 1986.

*Member, the American Ceramic Society.

*Present address: IBM Almaden Research Center, San Jose, CA 95120-6099.

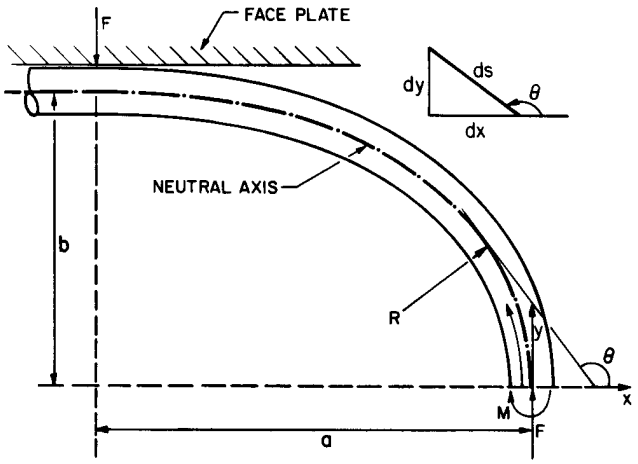

Fig. 2. Geometry of the bent fiber.

reducing the effective fiber diameter. This last problem can be eliminated by stripping the coating material before testing.

(ii) For strong fibers (strain to failure $\gtrsim 1\%$) the linear elastic analysis for the bend geometry becomes inaccurate since it assumes small strains. However, the results are still qualitatively correct, though quantitatively the error in the predictions increases with increasing strain (i.e., strength).

(iii) The tested length of fiber in bend is very small and therefore bending results are not useful for inferring the strength statistics of kilometer lengths of fiber.

(iv) The mean strength of a material depends on the specimen size because of the stochastic nature of the distributions in position and size of strength-reducing defects; the larger the specimen, the greater the probability of finding a larger defect. In tension it is possible to predetermine the length of fiber that is to be tested; however, this is not the case for bending as the length of bent fiber depends on the radius of curvature at fracture and hence on the strength. Also, the strength depends on the tested length, which itself depends on the strength! A correction for this effect must be made before quantitative comparisons can be made between bend data for fibers of different strengths and between bend and tensile data for the same fiber.

The purpose of the work described here is to examine these last points in detail and to directly compare strength measurements made in tension and bending.

II. Analysis

(1) Geometry of the Bend

The stress distribution around the bent fiber must be known before the strength of the fiber can be determined from the faceplate separation at fracture. Gulati[4] presented an analysis of the bend which is described below. France *et al.*[3] independently analyzed the bend, and their results agree with those of Gulati, though little detail of the analysis is given.

Figure 2 defines the geometry of the bend and the coordinate system that will be used. The radius of curvature, R, at the point (s, θ) is given by

$$d\theta/ds = 1/R \tag{1}$$

Taking moments about this point and using the well-known bending beam equation we have

$$EI\frac{d\theta}{ds} = -Fx - M \tag{2}$$

where F and M are the force and moment acting on the fiber, as defined in Fig. 2. Differentiation with respect to s gives

$$\frac{d^2\theta}{ds^2} = -\frac{F}{EI}\frac{dx}{ds} \tag{3}$$

where E is the Young's modulus of the fiber and I the second moment of cross-sectional area. Using the relations

$$dx/ds = -\cos\theta \tag{4a}$$

$$dy/ds = \sin\theta \tag{4b}$$

we find

$$\frac{d^2\theta}{ds^2} = \frac{F}{EI}\cos\theta \tag{5}$$

which is readily integrated to give

$$\frac{d\theta}{ds} = \left(\frac{2F\sin\theta}{EI}\right)^{1/2} \tag{6}$$

after application of the boundary condition that $1/R = d\theta/ds = 0$ when $\theta = \pi$. This equation may now be integrated to find the various shape parameters which describe the size of the bend:

$$a = -\int_{\pi/2}^{\pi} ds\cos\theta = 2^{1/2}\left(\frac{EI}{F}\right)^{1/2} = 1.414\left(\frac{EI}{F}\right)^{1/2} \tag{7a}$$

$$b = \int_{\pi/2}^{\pi} ds\sin\theta = \frac{\mathcal{J}(1/2)}{2^{1/2}}\left(\frac{EI}{F}\right)^{1/2} = 0.847\left(\frac{EI}{F}\right)^{1/2} \tag{7b}$$

$$L = \int_{\pi/2}^{\pi} ds = \frac{\mathcal{J}(-1/2)}{2^{1/2}}\left(\frac{EI}{F}\right)^{1/2} = 1.854\left(\frac{EI}{F}\right)^{1/2} \tag{7c}$$

where L is the half-length of the bend section of fiber and where $\mathcal{J}(x)$ is the integral defined by

$$\mathcal{J}(x) = \int_0^{\pi/2}\sin^x\psi\,d\psi = \int_0^{\pi/2}\cos^x\psi\,d\psi = \frac{\pi^{1/2}}{2}\frac{\Gamma\left(\frac{x+1}{2}\right)}{\Gamma\left(\frac{x+2}{2}\right)} \tag{8}$$

in which $\Gamma(x)$ is the gamma or factorial function defined by

$$\Gamma(x) = \int_0^{\infty}\xi^{x-1}e^{-\xi}\,d\xi \tag{9}$$

which is readily calculated using polynomial approximations.[5] The stress on the outer surface of the fiber (one fiber radius, r, from the neutral axis) is

$$\sigma = (r/R)E \tag{10}$$

and hence

$$\sigma(\theta) = r[(2EF/I)\sin\theta]^{1/2} \tag{11}$$

The maximum tensile stress, σ_{max}, occurs at $\theta = \pi/2$ and is

$$\sigma_{max} = r(2EF/I)^{1/2} \tag{12}$$

The faceplate separation at fracture, D, is given by

$$D = 2b + d$$

where d is the overall fiber diameter (including any coating material so that in general $d \neq 2r$). Hence from Eqs. (7(*b*)) and (12), at fracture

$$\sigma_{max} = 1.198E\frac{2r}{D-d} \tag{13}$$

It should be noted that the maximum stress is $\approx 20\%$ higher than is given by the simple first-order analysis which predicts that the fiber is bent into a semicircle. The calculated value of the numerical factor in Eq. (13) agrees quite well with the value of 1.24 ±

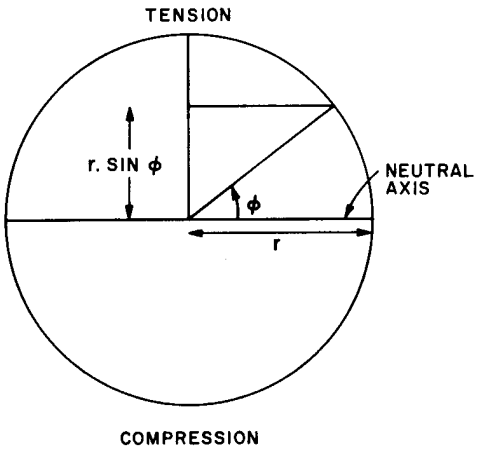

Fig. 3. Section through the bent fiber.

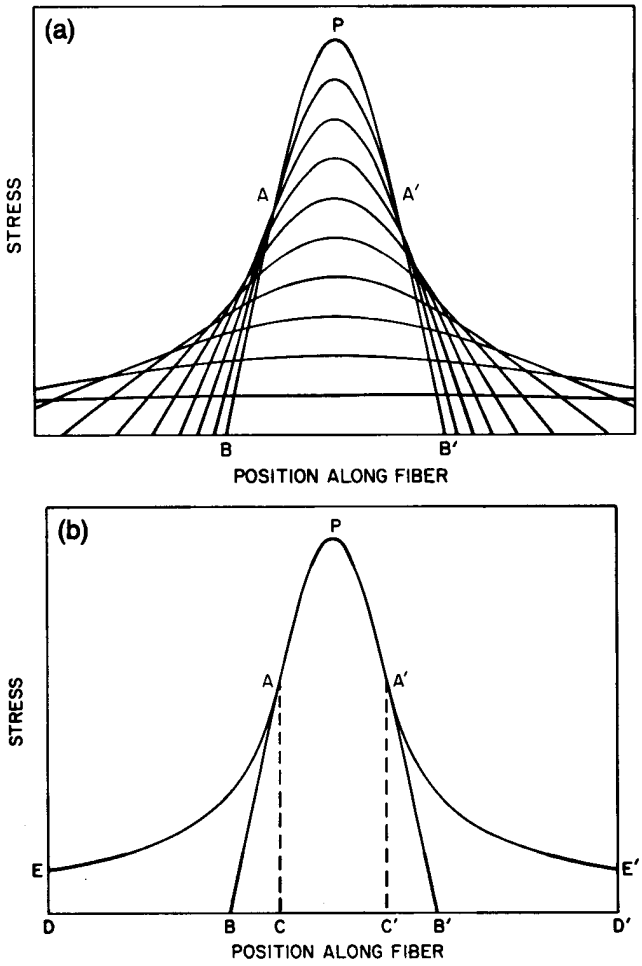

Fig. 4. (*a*) Stress profiles as the fiber is progressively loaded. (*b*) Final stress profile and maximum stress envelope.

0.04 obtained by direct measurement of faceplate separations and fiber bend radii.[6]

At this point in his analysis Gulati gave an order-of-magnitude estimate of the effective length of fiber that would have to be stressed in uniaxial tension in order to give the same strength as the bend experiment for fibers with a particular distribution of strengths. The next section presents a general analysis for the equivalent tensile length for fibers of general strength distribution.

(2) Test Length Considerations

In this section an analysis is presented which corrects for the fact that the length of fiber stressed in bending depends upon its strength. The results can then be used to predict tensile strengths from bend strength results or vice versa.

Weakest-link theory gives the result that the cumulative probability of failure by a representative stress, σ', is given by

$$F(\sigma') = 1 - \exp\left[-\int_A f(\sigma)\, dA\right] \tag{14}$$

where $f(\sigma)$ is interpreted as the probability per unit (small) area that failure has occurred by a stress σ. Since, in general, σ is a function of position, $f(\sigma)$ must be integrated over the entire specimen surface. σ' is a parameter which represents the magnitude of the stress field and would be the applied stress in a tensile experiment or σ_{max} for a bending experiment. The form of $f(\sigma)$ is not known a priori and any suitable function may be arbitrarily chosen. The most commonly used form for $f(\sigma)$ is the Weibull distribution because of its wide applicability and ease of use.

$$f(\sigma)\, dA = \left(\frac{\sigma(\mathbf{r})}{\sigma_0}\right)^m \frac{dA}{A_0} \tag{15}$$

The factor A_0 is not usually included in this expression but is used here to retain dimensional consistency in Eq. (14). A_0 may be taken as magnitude unity in the current system of units; σ_0 is then a measure of the strength of specimens with unit surface area. If the factor A_0 is omitted, σ_0 would not have dimension [stress] but [stress] [area]$^{1/m}$—a parameter whose dimensionality is hard to interpret!

The three-parameter Weibull distribution, which incorporates a threshold stress below which failure will not occur, is not used here since the added complexity is not justified. While an improved fit to experimental data would be obtained, this is a result of increased "flexibility" provided by a third variable parameter rather than an improved physical description of the data. Also, the possibility of very low strengths in very long length fibers should not be precluded since they are observed in practice.

For the bent fiber $\sigma(\mathbf{r}) = \sigma(\theta, \phi)$ where θ represents position along the fiber (Fig. 2) and ϕ represents position around the fiber circumference (Fig. 3). Therefore from Eqs. (11), (12), and (15) we have

$$f(\sigma)\, dA = \left(\frac{\sigma_{max}}{\sigma_0}\right)^m \sin^{m/2}\theta \sin^m\phi\, ds\, r\, d\phi \frac{1}{A_0} \tag{16}$$

but from Eqs. (6) and (12)

$$ds = d\theta\left(\frac{EI}{2F\sin\theta}\right)^{1/2} = \frac{Er}{\sigma_{max}\sin^{1/2}\theta}\, d\theta \tag{17}$$

and hence

$$\int_A f(\sigma)\, dA = \frac{\sigma_{max}^{m-1}}{\sigma_0^m}\frac{Er^2}{A_0}\int_0^\pi \sin^{(m-1)/2}\theta\, d\theta \int_0^\pi \sin^m\phi\, d\phi$$

$$= \frac{4Er^2}{A_0\sigma_0^m}\mathcal{J}\left(\frac{m-1}{2}\right)\mathcal{J}(m)\sigma_{max}^{m-1} \tag{18}$$

The equivalent expression for a tensile test is

$$\int_A f(\sigma)\, dA = \frac{2\pi rl}{A_0}\frac{1}{\sigma_0^m}\sigma^m \tag{19}$$

Comparing Eqs. (18) and (19) we see that the distribution of strengths in bending is still Weibull in form but with a modified Weibull exponent.

(3) Correction for Prestressed Sections of Fiber

The preceding analysis provides only an approximate evaluation of the failure probability of the bent fiber. Consider Fig. 4(*a*), which shows the distribution of stress along the fiber at successive positions as the faceplates are brought together. If the fiber breaks

when the bent section is BB', then the stress profile along the fiber is $BAPA'B'$. Consider now Fig. 4(b), which shows this stress profile $BAPA'B'$ and also the envelopes, AE and $A'E'$, of all stress profiles encountered during the previous loading. We see that the sections of fiber BC and $C'B'$ have been under a higher stress at some stage in the past and that sections BD and $D'B'$ and beyond, while now under zero stress, have been stressed in the past, and have survived this prestressing. Clearly, when evaluating the risk function of Eq. (15), the appropriate stress profile to use is $EAPA'E'$ rather than $BAPA'B'$. The first step in this analysis is to locate the points C and C'. From Fig. 4(a) it is seen that the stress in the fiber section CC' increases when the faceplates are brought together by a small amount, while the stress in sections BC and $C'B'$ decreases. C and C' are defined as the positions at which the stress does not change as the faceplates are moved; that is

$$\left.\frac{\partial}{\partial b}\sigma(s,b)\right|_s = 0 \tag{20}$$

When the expression for $\sigma(\theta)$ of Eq. (11) is substituted into Eqs. (7(b)) and (20), we find

$$\frac{\sin\theta}{b} = \frac{\cos\theta}{2}\frac{d\theta}{db} \tag{21}$$

Equations (6) and (7(b)) on integration give

$$\frac{s}{b} = \frac{1}{\mathcal{J}(\frac{1}{2})}\int_{\pi/2}^{\theta}\frac{d\psi}{\sin^{1/2}\psi} \tag{22}$$

which when differentiated with respect to b, holding s constant, gives

$$\frac{d\theta}{db} = -\mathcal{J}(\tfrac{1}{2})\frac{s}{b^2}\sin^{1/2}\theta \tag{23}$$

Combining Eqs. (21), (22), and (23), we obtain

$$\int_{\pi/2}^{\theta}\frac{d\psi}{\sin^{1/2}\psi} = -\frac{2\sin^{1/2}\theta}{\cos\theta} \tag{24}$$

The particular value of θ, θ_0 say, which satisfies this equation defines the positions of C and C'. θ_0, found numerically, is 157.101°.

The risk of failure for the section of fiber between C and C' is obtained by modifying the θ integration of Eq. (18) to be between the limits $(\pi-\theta_0, \theta_0)$ giving

$$\int_{CC'} f(\sigma)\,dA = \frac{4Er^2}{A_0\sigma_0^m}\mathcal{J}((m-1)/2,\theta_0)\mathcal{J}(m)\sigma_{max}^{m-1} \tag{25}$$

Table I. Comparison of the Slopes and Intercepts of the Straight Lines Obtained for Bending and Tension on a Weibull Probability Plot

	Slope	Intercept
Bending	$m-1$	$\ln[4Er^2\mathcal{M}(m)\mathcal{J}(m)/A_0\sigma_0^m]$
Tension	m	$\ln(2\pi rl/A_0\sigma_0^m)$

where

$$\mathcal{J}(x,\psi) = \int_{\pi/2}^{\psi}\sin^x\xi\,d\xi \tag{26}$$

$$\rightarrow \mathcal{J}(x) = \mathcal{J}(x,\pi)$$

Now we may find the stress distribution corresponding to the envelopes EA and $A'E'$ of Fig. 4(b). From Eq. (20) we deduce that the maximum stress that any part of the fiber in the region DC and $C'D'$ has seen occurs when it was at a position corresponding to θ_0 at some larger faceplate separation. Since this position is defined by Eq. (22) to be

$$s/b = \mathcal{J}(-\tfrac{1}{2},\theta_0)/\mathcal{J}(\tfrac{1}{2}) \tag{27}$$

we have from Eqs. (11) and (7(b))

$$\sigma(s) = \frac{Er\mathcal{J}(-\frac{1}{2},\theta_0)}{s}\sin^{1/2}\theta_0 \tag{28}$$

and hence the complete distribution around the fiber circumference is

$$\sigma(s,\phi) = \frac{Er\mathcal{J}(-\frac{1}{2},\theta_0)}{s}\sin^{1/2}\theta_0\sin\phi \tag{29}$$

and the contribution to the failure probability is

$$\begin{aligned}\int_{EC,C'E'} f(\sigma)\,dA &= \left(\frac{Er\mathcal{J}(-\frac{1}{2},\theta_0)\sin^{1/2}\theta_0}{\sigma_0}\right)^m \\ &\quad\times\int_0^{\pi}\sin^m\phi\,d\phi\,\frac{r}{A_0}2\int_{s_0}^{\infty}\frac{ds}{s^m} \\ &= 4\left(\frac{Er\mathcal{J}(-\frac{1}{2},\theta_0)\sin^{1/2}\theta_0}{\sigma_0}\right)^m \\ &\quad\times\mathcal{J}(m)\frac{r}{A_0}\frac{1}{(m-1)s_0^{m-1}}\end{aligned} \tag{30}$$

where s_0 is the position of C. From Eq. (28) it may be deduced that σ_{max}, the stress at $\theta = \pi/2$ at fracture, is given by

$$\sigma_{max} = Er\mathcal{J}(-\tfrac{1}{2},\theta_0)/s_0$$

which may be used to eliminate s_0 from Eq. (30) giving

$$\int_{EC,C'E'} f(A)\,dA = \frac{4Er^2}{A_0\sigma_0^m}\frac{\mathcal{J}(-\frac{1}{2},\theta_0)\sin^{m/2}\theta_0\mathcal{J}(m)}{m-1}\sigma_{max}^{m-1} \tag{31}$$

This equation has the same dependence on σ_{max} as the contribution from the central section of the fiber (Eq. (25)) so that the strength distribution is still Weibull in form.

Table I summarizes the slopes and intercepts for bending and tension for the Weibull plot of ln ln $[1/(1-F)]$ vs ln (stress). The function $\mathcal{M}(m)$ in the intercept may be calculated exactly or good approximations can be made. Table II compares the exact expression with two approximate ones. The exact expression involves evaluation of $\mathcal{J}(x,\psi)$ which must be done numerically. Approximation 1, the analysis presented in the previous section, avoids this computation. The expression underestimates $\mathcal{M}(m)$ by an amount corresponding to the regions bounded by $EABD$ and

Table II. Comparison of the Exact Form for $\mathcal{M}(m)$ with Two Approximate Forms

	$\mathcal{M}(m)$	Stress profile (Fig. 4(b))	Comments
Exact	$\mathcal{J}((m-1)/2,\theta_0) + [\mathcal{J}(-\frac{1}{2},\theta_0)\sin^{m/2}\theta_0]/(m-1)$	$EAPA'E'$	Inconvenient to calculate $\mathcal{J}((m-1)/2,\theta_0)$
Approx. 1	$\mathcal{J}((m-1)/2)$	$BAPA'B'$	Underestimate; better than approximation 2 for $m \gtrsim 3$
Approx. 2	$\mathcal{J}((m-1)/2) + [\mathcal{J}(-\frac{1}{2},\theta_0)\sin^{m/2}\theta_0]/(m-1)$	$EA + A'E' + BAPA'B'$	Overestimate; better than approximation 1 for $m \lesssim 3$

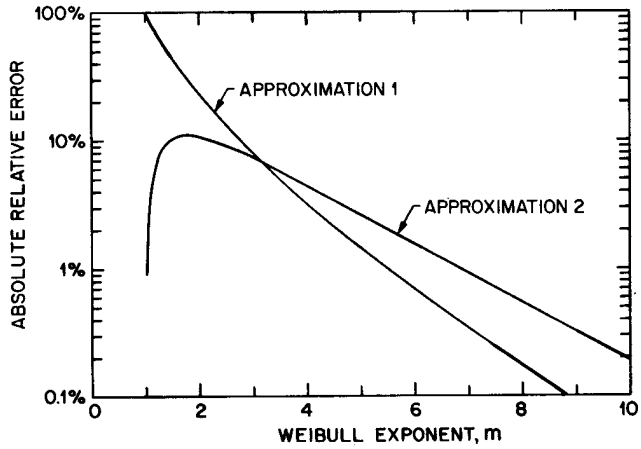

Fig. 5. Absolute relative error as a function of the Weibull exponent, m, for the two approximate expressions for the function $\mathcal{M}(m)$ given in Table II.

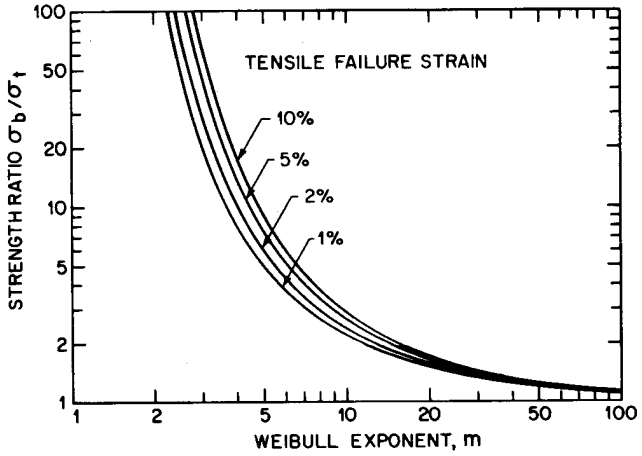

Fig. 6. Variation of the bending and tensile strength ratio with Weibull exponent, m, for four different strength fibers.

$E'A'B'D'$ in Fig. 4(b). Approximation 2 only involves calculating $\mathcal{J}(-\frac{1}{2}, \theta_0)$ (=1.354 30) and overestimates $\mathcal{M}(m)$ by an amount corresponding to regions BAC and $B'A'C'$.

Figure 5 shows the absolute value of the relative errors involved in these two approximations. For $m \geq 3$, approximation 1 is better than approximation 2 and the error is negligible for $m \geq 5$. Therefore, for most circumstances in which m takes moderate or large values, approximation 1, which is significantly easier to calculate than the exact expression, provides adequate accuracy. However, all results presented here incorporate exact calculations of the function $\mathcal{M}(m)$.

(4) Mean Strengths in Bending and Tension

The mean strength associated with a distribution of the form

$$F(\sigma) = 1 - \exp[-(\sigma/\sigma')^m]$$

is given by

$$\bar{\sigma} = \sigma'\Gamma(1 + 1/m)$$

and hence the mean strength for bending, σ_b, is given by

$$\sigma_b = \left(\frac{A_0\sigma_0}{4Er^2I\mathcal{M}(m)\mathcal{J}(m)}\right)^{1/(m-1)} \sigma_0\Gamma[1 + 1/(m - 1)] \tag{32}$$

while the mean strength for tension, σ_t, is

$$\sigma_t = \left(\frac{A_0}{2\pi rl}\right)^{1/m} \sigma_0\Gamma(1 + 1/m) \tag{33}$$

The ratio of these two quantities may be expressed as

$$\frac{\sigma_b}{\sigma_t} = \left\{\frac{\sigma_t}{E}\frac{l}{r}\frac{\pi}{2}\frac{1}{\mathcal{M}(m)\mathcal{J}(m)}\frac{\Gamma^{m-1}[1 + 1/(m - 1)]}{\Gamma^m(1 + 1/m)}\right\}^{1/m-1} \tag{34}$$

and hence is a function of the strain at failure in tension (σ_t/E), the tensile specimen aspect ratio (l/r) and the Weibull exponent, m.

Figure 6 compares the ratio of strengths in bending and tension for a 125-μm-diameter fiber, with a 1-m length in tension, as a function of the Weibull exponent, m, for various failure strains. The ratio of the strengths is near unity for large m but for small m the strength in bending diverges. This effect is just due to the differing test lengths—the mean strengths of two fibers of length l_1 and l_2 are in ratio $(l_2/l_1)^{1/m}$ and for large m this factor is close to unity; however, for small m the factor can be significant, as it is when comparing bending with tension.

Using rough approximations, Gulati[4] estimated bending to tensile strength ratios of 1.25 for $m = 46$ and 1.04 for $m = 200$. The above analysis gives values of 1.25 and 1.06 assuming a tensile strength of 5% strain in a 1-m length, which are in good agreement.

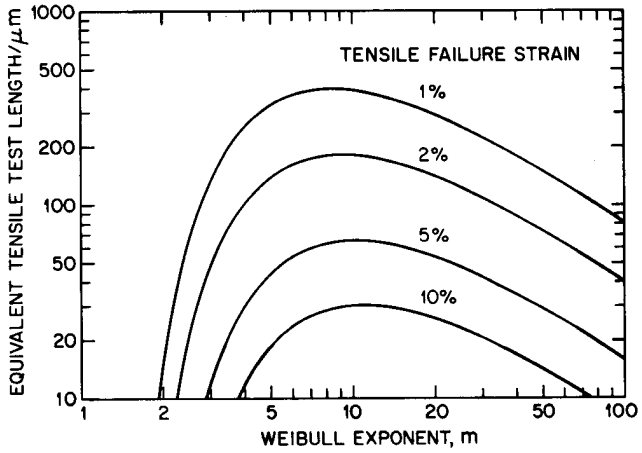

Fig. 7. Variation of the equivalent tensile test length with Weibull exponent, m, for four different strength fibers.

(5) Equivalent Tensile Test Length

We will now consider the equivalent length of fiber that would have to be tested in tension to give the same mean strength as measured in the bend test. Equating the mean strengths in bending and tension we find that the equivalent tensile length is given by

$$l_t = \left\{\frac{r}{l_0^{1/m}}\frac{E}{\sigma_t}\frac{2}{\pi}\mathcal{M}(m)\mathcal{J}(m)\frac{\Gamma^m(1 + 1/m)}{\Gamma^{m-1}[1 + 1/(m - 1)]}\right\}^{m/(m-1)} \tag{35}$$

where σ_t is the tensile strength of the fiber at some constant length l_0. Figure 7 shows the variation of l_t with m for four different fiber strengths (σ_t/E) assuming a tensile test length of $l_0 = 1$ m. The equivalent length has a maximum value, but is small for both small and large m. At large m, the probability of failure, which is proportional to the m-th power of stress, falls very rapidly with distance from the position of maximum stress at the tip of the bend. Therefore, only a very small part of the surface has a significant probability of fracture and the equivalent length is small. At small m, the bending strength is very high (see Fig. 6) and so the amount of fiber in the bend is very small, leading again to a small equivalent length.

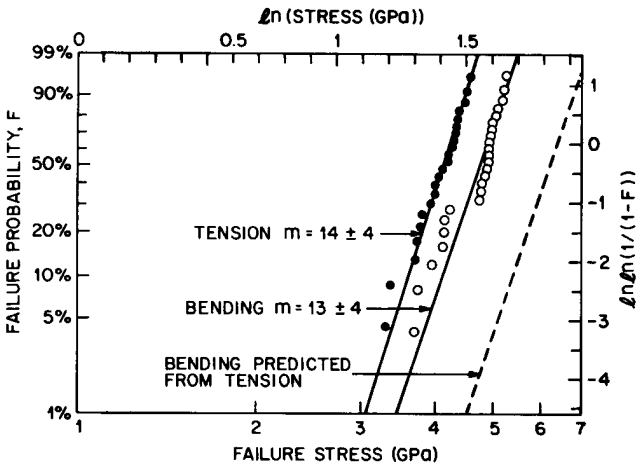

Fig. 8. Weibull probability plot of bending and tensile data for an intermediate-m-valued fiber. The dashed line is the bending behavior that would be predicted from the tensile results.

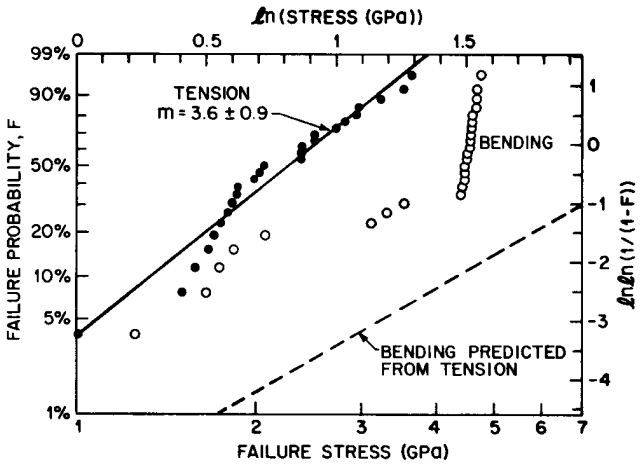

Fig. 9. Weibull probability plot of bending and tensile data for a low-m-valued fiber. The dashed line is the bending behavior that would be predicted from the tensile results.

To summarize Fig. 7, for all reasonable values of m and fiber strength, the equivalent tensile length is between 10 and 1000 μm. This is typically 3 orders of magnitude smaller than the length of specimen usually used in tension. It is also much smaller than the length of bent fiber, and significant errors would be introduced if it were assumed that the fiber were bent into a semicircle.

III. Experimental Results

The bending and tensile methods described in Section I have been used to measure the strengths of three silica fibers with representatively large, intermediate, and small values for their Weibull exponents and the preceding analysis has been used to correlate the results of the two techniques. In all cases the fiber diameter (excluding the polymeric coating) was 125 μm, the tensile test length was 25 mm, and the coating material was stripped before breaking the fibers in bending.

(1) Intermediate-Weibull-Exponent Fiber

Figure 8, a Weibull probability plot, compares the bending (open circles) and tensile (closed circles) data for the intermediate-Weibull-exponent fiber—the measured values of m for the two sets of data are marked and were calculated using an unbiased maximum likelihood estimator technique[7] which also provides the confidence limits which here represent a 90% confidence interval. The Weibull parameters are more usually determined by finding the best-fit straight line to the data on the Weibull probability plot. This type of linear regression makes invalid assumptions about the data and, while the expectation values of the Weibull parameters do not differ significantly from the maximum likelihood estimates, the confidence intervals are systematically grossly underestimated. For example, linear regression gives a value of $m = 12.3 \pm 0.7$ for the tensile data of Fig. 8, while the unbiased maximum likelihood estimator is 14 ± 4 for the same 90% confidence interval.

The estimated values of m for tension and bending are in good agreement and, as expected, the bend strength is significantly higher than the tensile strength. However, the dashed line shows the behavior in bending that is predicted from the tensile data but the agreement with the experimental bending data is poor. The median failure strain for this fiber is $\approx$6% and from Fig. 7 the equivalent tensile length is $\approx$50 μm compared with the tensile test length of 25 cm. Clearly with such a large difference in tested length, and with such a broad distribution of strength, the two experiments explore quite different regions of the flaw size distribution. The Weibull distribution corresponds to a unique flaw size distribution;[8] since the Weibull distribution is arbitrary, so is the flaw size distribution and so it cannot be expected that extrapolation from one part of the distribution to another will give reliable results.

(2) Low-Weibull-Exponent Fiber

Figure 9 compares bending and tensile results of the low-m-value fiber. The tensile data give a value of $m \simeq 4$, while the bending data give a bimodal strength distribution. The low-strength mode probably corresponds to the strengths observed in tension, but the high-strength mode is not observed at all in tension. Again, the bending behavior predicted from the tensile data (dashed line) does not correspond to the observed behavior.

The criterion for bimodality used here is that the Weibull exponents for the two modes should be significantly different from both each other and the single Weibull exponent obtained assuming a unimodal distribution. The tensile data do satisfy this criterion, while the bending data do not.

It should be noted that the predicted bending strength distributions in Figs. 8 and 9 both give median strengths in excess of 6 GPa which is unphysical since the maximum observed strength of this type of fiber is of this order. The Weibull distribution predicts that the mean strength of a specimen increases as its size decreases and for an arbitrarily small specimen the strength may be arbitrarily large. In reality the strength of a specimen cannot exceed the theoretical strength of the material. This behavior is incorporated neither in the Weibull distribution nor in other commonly used distributions.

(3) High-Weibull-Exponent Fiber

At high values of m one expects the agreement between predicted and observed behavior to be better because test length changes are less important. Figure 10 shows typical results for an as-drawn high-strength fiber. In this case, while there is good agreement between the measured values of m, the bending strength is lower than the tensile strength while it is predicted to be higher (dashed line). This behavior could be explained by the nonlinearity of the Young's modulus of silica. At this strain level ($\approx$8%) the modulus of silica is $\approx$94 GPa compared with $\approx$72 GPa at zero strain.[9] If this higher value of modulus is used, the bending data have a median strength approaching 8 GPa, which is higher than the predicted strength. The effective modulus will lie between 72 and 94 GPa because the strain in the bent fiber varies between 0 and 8%. A more detailed calculation involving a stress-dependent modulus is not justified since at 8% strain the linear elastic analysis for the bend geometry becomes unreliable. However, while the agreement between the observed and predicted median strengths in bending is not good, the values are not inconsistent.

Kurkjian and Paek[10] found that for as-drawn high-strength fibers the *apparent* variability in strength approximately equals the vari-

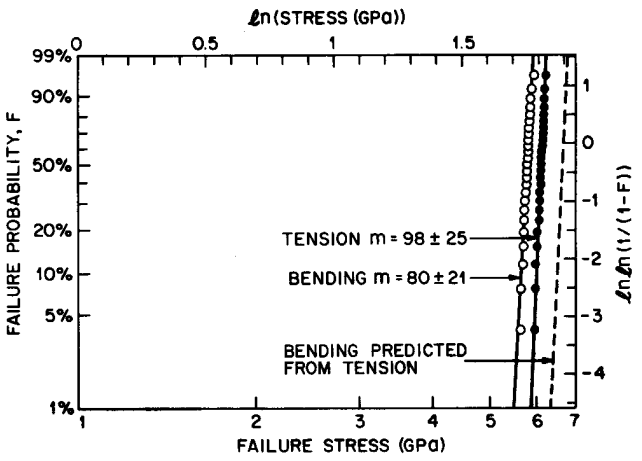

Fig. 10. Weibull probability plot of bending and tensile data for a high-m-valued fiber. The dashed line is the bending behavior that would be predicted from the tensile results.

ability in cross-sectional area of the fiber caused by diameter fluctuations. They concluded that the *real* variability in strength does not contribute significantly to the measured variability. The fluctuations in fiber diameter will depend on the details of the feedback system used to control the diameter of the fiber in the drawing process as well as the draw speed.

Measurements of fiber diameter for a typical fiber drawn at 1 ms^{-1} showed large-scale variation in diameter of ≈2-m length and a variable amplitude with a maximum peak-to-peak distance of ≈1 μm. Superimposed upon this were smaller fluctuations with characteristic length of up to 10 cm and peak-to-peak amplitude ≈0.2 μm. The periodic fluctuations are thought to be characteristic of the feedback parameters of the diameter control mechanism while the small-scale fluctuations are due to background noise and are possibly dependent on the physical properties of silica glass. Such complex behavior makes it impossible to make a priori predictions of length effects from diameter variation statistics since these will vary from fiber to fiber. Thus, the close agreement between the tensile and bending values of the Weibull exponent for the high-m fiber is merely fortuitous. Note that the agreement is not due to both methods sampling similar diameter distributions. If it is assumed that fluctuations in perpendicular diameters correlate (i.e., the fiber retains circularity through fluctuations), then apparent strength variability for the tensile test depends on variability in the square of the diameter, while for the bending method it depends on the cube.

IV. Discussion and Conclusions

The bending technique for evaluating the strength of optical fibers has been described and has proved to be very useful in situations where a tensile technique is unsuitable. An analysis which may be used to compare tensile and bending data has been presented and shows that the effective length of fiber that is stressed in bending is very small compared to tensile test lengths and also to the length of bent fiber. For this reason, except for fibers with a very narrow distribution of strengths (large Weibull exponent), the agreement between bending and tensile results is poor since quite different sections of the flaw size distributions are explored by the two methods. For large-Weibull-exponent fibers the agreement is still not good because variability in apparent strength is due to variability in the fiber diameter. Much better agreement between predictions and experiment would be realized for a low-strength (strain to failure ≤1%) high-Weibull-modulus fiber, but such a material is not available.

It should be noted that the analysis for the effect of tested length presented here relies on the assumption that the fiber strengths follow the Weibull distribution. Other distribution functions may be used and would give different predictions which may or may not agree better with the observed behavior. However, while a particular distribution function may in hindsight appear better than others, there is no reason to suppose that it will be better for other experiments. There are no sound physical models available at present for predicting strength distributions so any distribution function may be chosen arbitrarily (e.g., the Weibull distribution for its ease of use) and used as a vehicle for describing the local strengths and flaw sizes.

While the bending technique is very useful, it should not be used as a direct substitute for tensile testing without careful consideration of the equivalence of bending and tensile data. It can however be employed as a tool that is used in parallel with tensile testing to provide additional information about the flaw distribution in the fiber.

References

[1]D. Sinclair, "A Bending Method for Measurement of the Tensile Strength and Young's Modulus of Glass Fibers," *J. Appl. Phys.*, **21**, 380–86 (1950).
[2]D. A. Pinnow, F. W. Dabby, and I. Camlibel, "Tensile Strength of Borosilicate-Clad Fused-Silica-Core Fiber Optical Wave Guides," *J. Am. Ceram. Soc.*, **58** [5–6] 261 (1975).
[3]P. W. France, M. J. Paradine, M. H. Reeve, and G. R. Newns, "Liquid Nitrogen Strengths of Coated Optical Fibres," *J. Mater. Sci.*, **15**, 825–30 (1980).
[4]S. T. Gulati, "Nonlinear Bending of Strong Glass Fibers"; for abstract see *Am. Ceram. Soc. Bull.*, **60** [8] 862 (1981).
[5]M. Abramowitz and I. A. Stegun, Handbook of Mathematical Functions. Dover, New York, 1965.
[6]J. B. Murgatroyd, "The Strength of Glass Fibers, Part II—The Effect of Heat Treatment on Strength," *J. Soc. Glass Technol.* **28**, 388–405 (1944).
[7]D. R. Thoman, L. J. Bain, and C. E. Antle, "Inferences on the Parameters of the Weibull Distribution," *Technometrics*, **11** [3] 445–60 (1969).
[8]M. J. Matthewson, "An Investigation of the Statistics of Fracture"; in Strength of Inorganic Glass. Edited by C. R. Kurkjian. Plenum Press, New York, 1985.
[9]J. T. Krause, L. R. Testardi, and R. N. Thurston, "Deviations from Linearity in the Dependence of Elongation upon Force for Fibers of Simple Glass Formers and of Glass Optical Lightguides," *Phys. Chem. Glasses*, **20** [6] 135–39 (1979).
[10]C. R. Kurkjian and U. C. Paek, "Single-Valued Strength of 'Perfect' Silica Fibers," *Appl. Phys. Lett.*, **42** [3] 251–53 (1983). □